Separation of acoustic and hydrodynamic components of the velocity for a CFD-BEM hybrid method

R. Piscoya, M. Ochmann

University of Applied Sciences Berlin, Germany,
*Email: piscoya@tfh-berlin.de, ochmann@tfh-berlin.de*

Introduction

The acoustic far field from open turbulent flames can be determined by using the hybrid approaches of aeroacoustics. These methods calculate the near field with a Computational Fluid Dynamics (CFD) code and transfer the data to an acoustic solver [1]. In the present approach, the Boundary Element Method (BEM) is the acoustic solver used to determine the radiated sound. If the input velocity has a high hydrodynamic component, the sound field calculated by the BEM will be overestimated, since local non-propagating velocity fluctuations will be assumed to propagate with sound speed.

To eliminate the hydrodynamic component, techniques employing a Helmholtz-Hodge vector decomposition are used and applied in the time domain (e.g. in [2]). In this article, we propose a method which combines the Dual Reciprocity BEM in the frequency domain with a vector decomposition in order to eliminate the hydrodynamic part of the particle velocity.

Basic Idea

The sound radiation of an open turbulent flame can be determined using the standard BEM if the normal particle velocity u_n is known at a closed surface S that encloses the flame (see Fig. 1). This approach is valid if the medium outside S is quiescent.
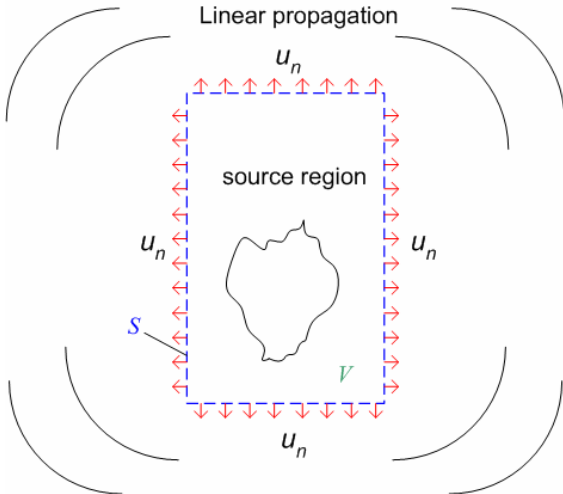
Figure 1: Illustration of the hybrid approach for the calculation of the radiation from flames.

The expression for the sound pressure radiated from the flame is given by the surface integral

$$C(\vec{x})p(\vec{x}) = \int_S \left(p(\vec{y})\frac{\partial g(\vec{x},\vec{y})}{\partial n(\vec{y})} + j\omega\rho\, u_n\, g(\vec{x},\vec{y}) \right) dS(\vec{y}). \quad (1)$$

where $g(\vec{x},\vec{y}) = \dfrac{e^{-jk|\vec{x}-\vec{y}|}}{4\pi|\vec{x}-\vec{y}|}$, $C(\vec{x}) = \begin{cases} 1 & \vec{x} \in V \\ 0.5 & \vec{x} \in S \\ 0 & \text{outside } V \end{cases}$

The values of the velocity can be provided by a compressible CFD calculation. CFD codes normally provide the data in time domain, but they can be converted to the frequency domain through a Fourier transform. A description of the processing of the data was given in [1].

The total velocity field obtained from the CFD is supposed to have not only an acoustic component, but also a hydrodynamic component that does not propagate with sound speed and decays with increasing distance to the burner nozzle. The amplitude of the non acoustic component is often bigger than the acoustic one. But if a sufficiently large control surface S is considered, it is expected that only the acoustic component is present and a BEM calculation can be started.

In many practical cases, the region where the hydrodynamic part is important is large and it may not be possible to extend the computational domain to cover it completely. For those cases, an alternative is to take a smaller control surface and separate the acoustic component from the hydrodynamic one. The control surface should be still large enough to enclose the real acoustic sources.

The total velocity field $\vec{v}$ can be written as a sum of three vector fields [3]:

$$\vec{v} = -\nabla\phi + \nabla \times \vec{A} + \vec{h} \quad (2)$$

where ϕ is a scalar potential, $\vec{A}$ a vector potential and $\vec{h}$ a "harmonic" vector with $\nabla \cdot \vec{h} = 0$ and $\nabla \times \vec{h} = 0$. The first vector describes an irrotational field since $\nabla \times \nabla\phi = 0$ and the second one a solenoidal field since $\nabla \cdot (\nabla \times \vec{A}) = 0$.

For low Mach numbers, where the fluid can be assumed as incompressible so that all compressible effects can be considered to have an acoustic nature, the acoustic velocity is entirely given by the first vector field:

$$\vec{u}^{(in)} = -\nabla\phi \quad . \quad (3)$$

Then, if we take the divergence of Eq. (2), we obtain a differential equation for the scalar potential ϕ.

$$\nabla^2\phi = -\nabla \cdot \vec{v} \quad . \quad (4)$$

Eq. (4) is a Poisson equation where the source term can be determined since the velocity is given. Once the scalar

potential is solved, the acoustic particle velocity can be derived from Eq. (3) and used as input for the BEM program.

For open turbulent flames, which are the focus of this work, it will be assumed that the error of neglecting the mean flow is small, since the Mach numbers are very low, especially at some distance from the burner nozzle. Under this assumption, the acoustic pressure inside S can still be defined in terms of the scalar potential ϕ

$$p^{(in)} \approx j\omega\rho\phi \tag{5}$$

To find a unique solution of Eq. (4), appropriate boundary conditions must be imposed. Since outside S the sound waves are assumed to propagate linearly, the sound pressure fulfils the homogeneous Helmholtz equation. In this region, pressure and particle velocity can be also defined in terms of a velocity potential ϕ',

$$p = j\omega\rho\phi' \quad , \quad \vec{u} = -\nabla\phi' \tag{6}$$

where ϕ' satisfies:

$$\nabla^2\phi' + k^2\phi' = 0 \tag{7}$$

Hence, requiring continuity of sound pressure and particle velocity at S and considering Eqs. (3), (5) and (6), the boundary conditions are given by:

$$\phi = \phi' \quad , \quad \frac{\partial\phi}{\partial n} = \frac{\partial\phi'}{\partial n} \tag{8}$$

Sound radiation in the far field

To evaluate (1), ϕ has to be previously determined at S. Applying the divergence theorem to Eq. (4) an integral equation for ϕ is obtained:

$$C(\vec{x})\phi(\vec{x}) = \int_S \left(\frac{\partial\phi(\vec{y})}{\partial n(\vec{y})} G(\vec{x},\vec{y}) - \phi(\vec{y})\frac{\partial G(\vec{x},\vec{y})}{\partial n(\vec{y})} \right) dS$$
$$- \int_V b(\vec{y})G(\vec{x},\vec{y})dV \tag{9}$$

$$b = -\nabla \cdot \vec{v} \quad , \quad G(\vec{x},\vec{y}) = \frac{1}{4\pi|\vec{x}-\vec{y}|} . \tag{10}$$

Using the Dual Reciprocity BEM (DRBEM), the volume integral in Eq. (9) can be expressed as a sum of surface integrals. In this method, the source b should be known in the volume enclosed by S so that an expansion of b in a set of functions f_j can be performed

$$b(\vec{x}) = \sum_j \alpha_j f_j \tag{11}$$

and a set of functions ψ_j satisfying the Poisson equation with f_j as a the source term must be found

$$\nabla^2\psi_j = f_j \tag{12}$$

Eq. (9) can be written as (see [4]):

$$C\phi = -\int_S \left(\phi\frac{\partial G}{\partial n} - \frac{\partial\phi}{\partial n}G \right) dS +$$
$$\sum_j \alpha_j \left(C\psi_j + \int_S \left(\psi_j \frac{\partial G}{\partial n} - \frac{\partial\psi_j}{\partial n}G \right) dS \right) \tag{13}$$

A second integral equation is obtained using the divergence theorem again for Eq. (7):

$$C'(\vec{x})\phi'(\vec{x}) = \int_S \left(\phi'(\vec{y})\frac{\partial g(\vec{x},\vec{y})}{\partial n(\vec{y})} - \frac{\partial\phi'(\vec{y})}{\partial n(\vec{y})} g(\vec{x},\vec{y}) \right) dS \tag{14}$$

where $C'=1-C$.

To solve Eqs. (13) and (14), both equations need to be discretized. If we generate a mesh of S with N elements and consider constant elements, i.e. the quantities are assumed to be constant over each element, the variables are solved at the center of each element.

The matrix forms of Eqs. (13) and (14) are then:

$$(0.5I + H^P)\phi^S = G^P \frac{\partial\phi^S}{\partial n} +$$
$$\left((0.5I + H^P)\psi^S - G^P \frac{\partial\psi^S}{\partial n} \right)\alpha \tag{15}$$

$$(0.5I - H^H)\phi'^S = -G^H \frac{\partial\phi'^S}{\partial n} \tag{16}$$

The matrices H^P, G^P, H^H and G^H are the usual $N{\times}N$ BEM system matrices. H^P and H^H have elements containing $\partial G/\partial n$ and $\partial g/\partial n$ respectively multiplied by a mesh element surface. G^P and G^H have elements containing the functions G and g respectively multiplied by a mesh element surface.

The coefficients α are determined directly from the known source term by discretizing Eq. (11).

$$\alpha = F^{-1}b \tag{17}$$

The matrix F is a $M{\times}M$ square matrix, where $M=N+L$ and L is the number of interior points considered in the discretization. The number of interior points should be at most of the order of N [5].

Eq. (16) provides a relation between ϕ' and $\partial\phi'/\partial n$. Taking into account the boundary conditions (8) a relation between ϕ and $\partial\phi/\partial n$ at the surface is also obtained which can be inserted in Eq. (15). Hence, a matrix equation for ϕ can be derived and solved:

$$\left(0.5I + H^P + G^P(G^H)^{-1}(0.5I - H^H) \right)\phi^S =$$
$$\left((0.5I + H^P)\psi^S - G^P \frac{\partial\psi^S}{\partial n} \right)\alpha \tag{18}$$

Numerical test

The procedure to separate the acoustic and hydrodynamic parts of the velocity was tested with a numerical example. Both velocity fields were conceived, the hydrodynamic part is divergence free as is required in this approach.

Acoustic Component

The acoustic component is given by a velocity field of a spherical source uniformly distributed within a radius R. Such configuration can be thought of a burning gas with a harmonic uniform heat release ratio (spherical flame). This case was investigated previously in [6].

The velocity field describing this source at all positions is given by

$$\vec{u}_n^{(in)} = \frac{S_\omega C j_1(k_0 r)}{k_0} \hat{r} \quad r \leq R$$
$$\vec{u}_n = k_0 A h_1^{(2)}(k_0 r) \hat{r} \quad r \geq R \tag{19}$$

Considering continuity of pressure and normal velocity at the boundary, the coefficients C and A are given by:

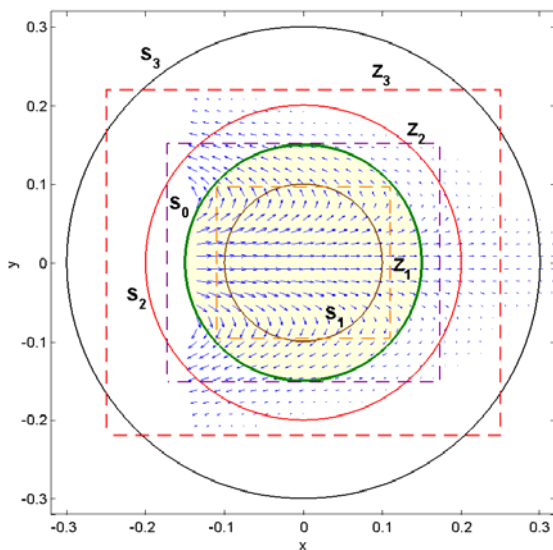$$C = jk_0^2 R^2 h_0'^{(2)}(k_0 R) \quad , \quad A = jS_\omega R^2 j_0'(k_0 R) \tag{20}$$

where S_ω is a constant describing the heat release ratio and j_0 and $h_0^{(2)}$ are the spherical Bessel and Hankel functions respectively.

Hydrodynamic Component

The non acoustic component of the total velocity is assumed to have the following expression:

$$\vec{v}_h = 2D\beta e^{-\rho^2/\tau^2}\left(1 - \frac{\rho^2}{\tau^2}\right)e^{-(x-d)/\beta} \hat{x} +$$
$$D\rho e^{-\rho^2/\tau^2} e^{-(x-d)/\beta} \hat{\rho} \tag{21}$$

for $x > d$. $\rho = \left(y^2 + z^2\right)^{1/2}$

Figure 2: Hydrodynamic component of the velocity and control surfaces.

This velocity is symmetric to the X-axis and each component decays exponentially in axial and radial directions. The constants τ and β determine how strong its magnitude decays. The parameter D allows adjusting the magnitude of the hydrodynamic velocity respect to the acoustic velocity.

In Fig. 2, the velocity vectors of (21) are shown as well as several control surfaces that were used to calculate the sound radiation. Two types of surfaces were used, cylinders (Z_1, Z_2 and Z_3) and spheres (S_0, S_1, S_2, S_3). The surface S_0 corresponds to the spherical flame surface with radius R. Inside S_0, the source exists, outside S_0 there are no acoustic sources. The form of the control surface has no influence on the sound field if the control surface encloses all acoustic sources.

Results

For the numerical calculations, the radius R was chosen to be 0.15 m. A model with 640 elements was used for the spherical control surfaces and a model with 768 elements for the cylinder. Both models have at least 6 elements per wavelength for frequencies up to 2000 Hz.

A first calculation of the sound radiation was made without applying the splitting technique. The sound power was determined using the total velocity at the control surface. The curves obtained with surfaces S_0, S_2, S_3, Z_2 and Z_3 are compared with the analytical sound power of the acoustic source and shown in Fig. 3.
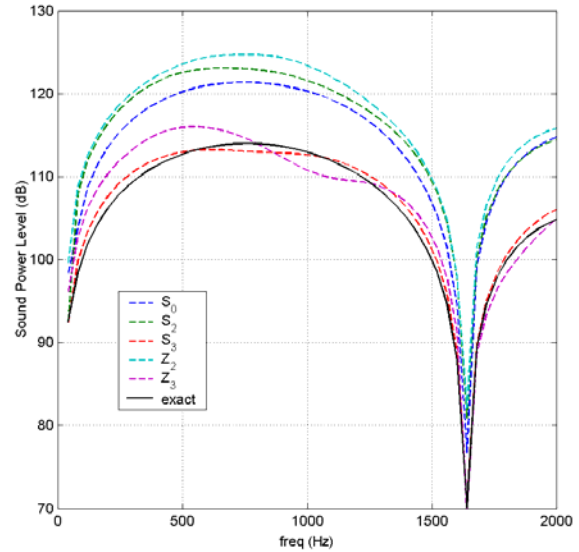
Figure 3: Sound power curves obtained with the BEM calculation using the total velocity field.

The sound power is clearly overestimated when the control surfaces lie in a region where the hydrodynamic part is important. For the larger surfaces S_3 and Z_3 the error is smaller because $\vec{v}_h$ has decayed.

The splitting technique was then tested. Eq. (18) was solved to find the scalar potential ϕ and its normal derivative $\partial\phi/\partial n$. The source term was given by

$$b = -\nabla \cdot \left(\vec{u} + \vec{v}_h\right) = -\nabla \cdot \vec{u}.$$

The expansion functions f_j in Eq. (11) are the radial functions suggested in [7]:

$$f_j(\vec{x}) = 1 + r_j \quad \text{with} \quad r_j = \left| \vec{x} - \vec{X}_j \right| \quad (22)$$

where $\vec{X}_j$ denotes the position of the j-th collocation point. Convergence properties of these functions are presented in the same work. The associated functions ψ_j of Eq. (12) and their derivatives are:

$$\psi_j(\vec{x}) = \frac{r_j^2}{6} + \frac{r_j^3}{12} , \quad (23.a)$$

$$\frac{\partial \psi_j}{\partial n} = \left(\frac{r_j}{3} + \frac{r_j^2}{4} \right) \frac{(\vec{x} - \vec{X}_j) \cdot \hat{n}}{\left| \vec{x} - \vec{X}_j \right|} , \quad (23.b)$$

The curves obtained with surfaces S_0, S_2, S_3, Z_2 and Z_3 are shown in Fig. 4, again compared with the exact solution.
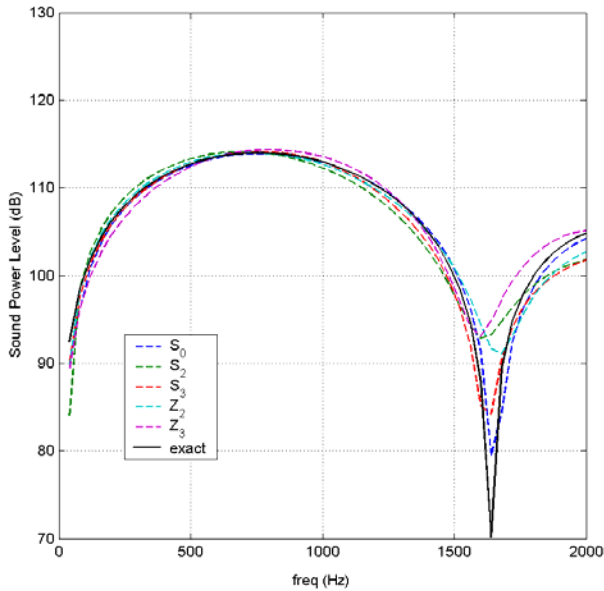
Figure 4: Sound power curves obtained with the BEM calculation applying the splitting technique.

Since all control surfaces enclose all acoustic sources, the sound power is expected to be the same. The agreement of the BEM curves obtained with the acoustic component alone is very good except near the first minimum of the sound power, where the error is expected to be bigger.

When the control surfaces S_1 and Z_1 are used, the results after using the splitting technique do not agree well with the exact solution, but that is expected since there are acoustic sources outside the control surfaces.

Conclusions

A method to separate the hydrodynamic and acoustic components of the velocity field provided from a compressible CFD calculation was presented. The method works in the frequency domain and is based on the DRBEM. This procedure is necessary if the velocity is used to compute the sound radiation of turbulent flames with a standard BEM calculation to avoid considering non propagating fluctuations.

The method was tested with a numerical example and has shown promising results. In a future work, the method will be applied to unsteady data of a LES calculation simulating a turbulent flame. Also, the inclusion of a mean flow will be considered.

References

[1] Piscoya R., Brick H., Ochmann M., Költzsch P., Equivalents Source Method and Boundary Element Method for Calculating Combustion Noise. Acta Acustica united with Acustica **94** (2008), 514-527

[2] De Roeck W., Baelmans M. and Desmet W., An aerodynamic/acoustic splitting technique for hybrid CAA applications, 13th AIAA/CEAS Aeroacoustics Conference (28th AIAA Aeroacoustics Conference), Rome, May 2007

[3] Batchelor, G. K., An Introduction to Fluid Dynamics, Cambridge University Press, 1967

[4] Piscoya R., Brick H., Ochmann M., Determination of the far field sound radiation from flames using the Duala Reciprocity Boundary Element Method. Acta Acustica united with Acustica (accepted)

[5] Duraiswami R., Sarkar K., Chahine G., Efficient 2D and 3D electrical impedance tomography using dual reciprocity boundary element techniques. Engineering Analysis with Boundary Elements **22** (1998), 13-31

[6] Piscoya, R., Ochmann, M., Schallabstrahlung einer kugelsymmetrischen Flamme, Fortschritte der Akustik, DAGA 2007, Stuttgart (2007)

[7] Partridge P.W., Brebbia C.A., Wrobel L.C., The dual reciprocity boundary element method. London, Elsevier, 1992